Automatic Image Mosaic System Using Steerable Harris Corner Detector

Mahesh
Research scholar, Department of ECE,
MITS, Madanapalle, AP, India
vka4mahesh@gmail.com

Subramanyam M .V.
Professor,Department of ECE
SREC, Nandyal, AP, India
mvsraj@yahoo.com

***Abstract*- Image mosaic is to be combine several views of a scene in to single wide angle view. This paper proposes the image mosaic based on feature based approach. The steps in image mosaic include feature point detection, feature point descriptor extraction and feature point matching. A RANSAC algorithm is applied to eliminate number of mismatches and obtain transformation matrix between the images. The input image is transformed with the correct mapping model for image stitching and same is estimated. In this paper, feature points are detected using steerable Harris and compared with traditional Harris, SUSAN corner detectors.**

***Keywords*- Image mosaic, corners features, RANSAC (**Random Sampling Consensus**), image stitching, Harris, SUSAN**

I. INTRODUCTION

Cameras don't have sufficient view angles to capture the surrounding scene in a single shot. The latest digital cameras with panorama facilities suffer from certain limitation, when camera and objects in the scene move in the same direction, the quality of the panorama image is degraded due to the effect of blurring or ghosting or both. If the camera is moved slower than specified speed, it results in failure of capturing complete panorama image. This paper is an attempt to address the above limitation of digital camera. The construction of large, high resolution image mosaics is an active area of research in photogrammetric fields, computer vision, image processing, and computer graphics. Image mosaic combines two or more images into a new wide angle image with as little distortion from the original images as possible. The stitched image can give a better vision on the scene when compared to the two images captured by two different angles. The first step in image stitching is to search for the overlap region or similarity within the images. This is done by extracting the feature points within the images using a feature point detector such as Harris[1], SUSAN[2,4] Kitchen and Rosenfeld[3], etc,. Then compare the feature points are to look for any matching pair. Based on the matching, transformation parameters are generated to transform the images into the same coordinate system that are agreed by each other. Finally, the images are ready to be stitched together.

This paper is organized as follows: The process of image stitching is explained in detail. In Section II, the basics of various feature point detectors are briefly described. Section III, explains the proposed method. The feature descriptors extraction and matching are briefly described in sections IV and V. The mosaic results are presented in Section VI. Finally, this paper is concluded in Section VII.

978-1-4673-2322-2/12/$31.00 ©2012 IEEE

II. FEATURE POINT DETECTION

Fig 1. shows image mosaic process flow, that is started by extracting the feature points in the two images. The feature detection contains significant structural information pixels. Feature point detection effects the success of feature matching. Different feature point detectors and their invariant

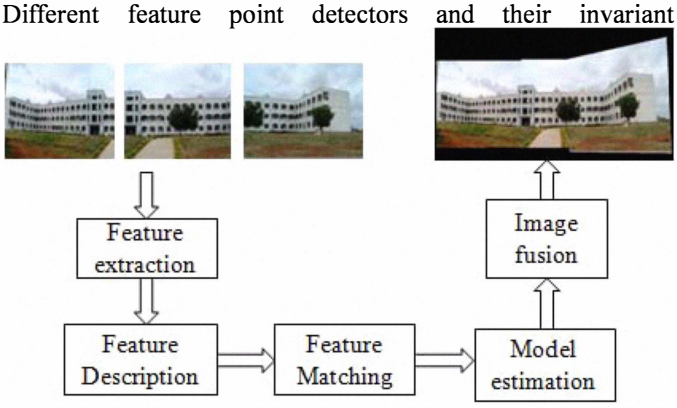

Figure1. Image mosaic process flow

A. *Harris Corner Detector*

In Harris detection algorithm calculating each pixel's gradient. If the absolute gradient value changes significant in all directions, then declare the pixel as a corner.

$$R = \det(M) - \lambda (trace(M))^2 \quad (1)$$

$$M = G(\sigma) * \begin{pmatrix} I_x^2 & I_x I_y \\ I_x I_y & I_y^2 \end{pmatrix} \quad (2)$$

R is measure the corner response at each pixel coordinates (x, y). λ is a constant and typical value is 0.04. I_x, I_y represents the first order gray gradient of horizontal and vertical, $G(\sigma)$ is an isotropic Gaussian filter with standard deviation σ and the operation * denotes convolution.

In Fig 2. λ_1, λ_2 is proportional to the principal curvatures of partial autocorrelation function. There, by judging the value of λ_1 and λ_2 to determine the slow changes of areas, corner and edge.

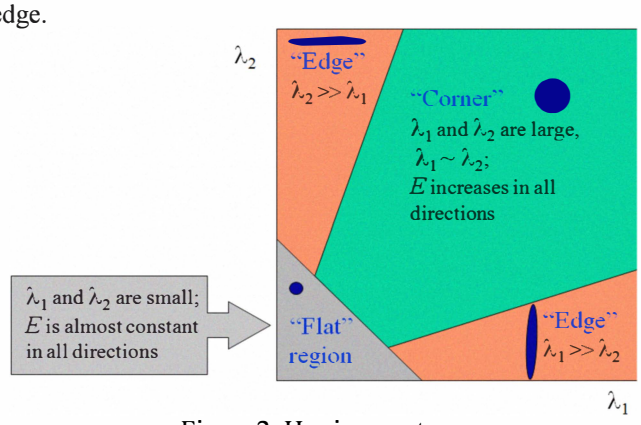

Figure 2. Harris operator

As per the gradient changes shown in Fig 2. are three cases[1] when the two curvatures are low this shows that local autocorrelation function is very flat, changes are not dramatic; If one curvature is low and the other is high, this means partial autocorrelation function changes in one direction means it's edge. When the two curvatures are high, indicating the local autocorrelation function has a peak, it's the corner. This is a fast and simple detector that partial invariant to noise, changes in illumination and rotation.

B. Susan Corner Detector

In the SUSAN detector a circular mask is applied around every pixel. If the greyscale values of all the pixels within the mask are compared to that of the centre pixel (the "nucleus"). All pixels with similar brightness to that of the nucleus are assumed to be part of the *Univalue Segment Assimilating Nucleus*: USAN.

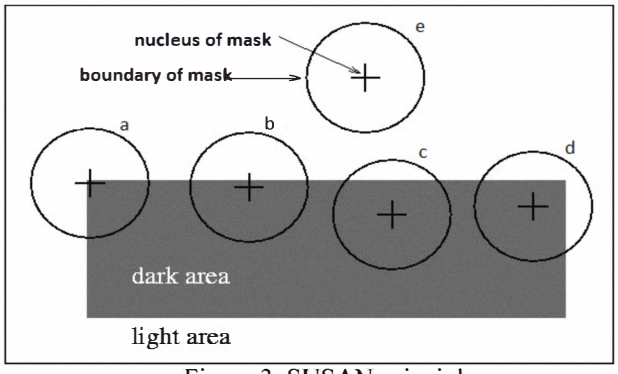

Figure 3. SUSAN principle

Consider Fig.3. showing a dark rectangle on a white background, five circular masks are shown at different positions on the simple image. Corners can be detected according to the area of USAN. Nucleus is on the corner when the area of USAN is up to the smallest, such as "a".

This corner detector computes fast, with good repeatability rate and invariant to noise.

C. Steerable filters

Steerable filters, introduced by Freeman and Adelson[5,6] are spatial oriented filters that can be expressed using linear combinations of a fixed set of basis filters. If the transformation is a translation, then the filter is said to be shiftable or steerable in position; if the transformation is a rotation, then the filter is said to be steerable in orientation or commonly steerable and the basis filters are normally called steerable basis filters. Given a set of steerable basis filters, we can apply them to an image and since convolution is linear, we can interpolate exactly, from the responses of the basis filters, the output of a filter tuned to any orientation we desire.

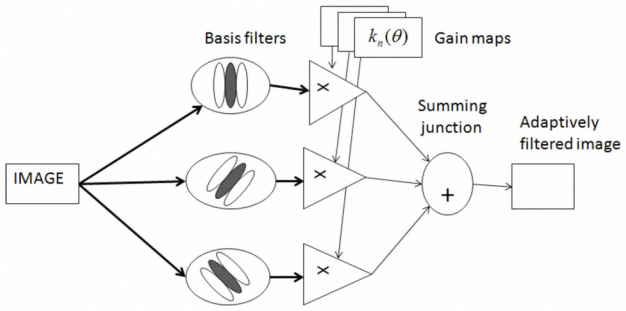

Figure 4. Steerable filter block diagram

The basic idea is to generate a rotated filter from a linear combination of a fixed set of basis filters. Fig 4. shows a general architecture for steerable filters, which consists of a bank of permanent, dedicated basis filters that always convolve the image as it comes in. The outputs are multiplied by a set of gain masks, which apply the appropriate interpolation functions at each position and time. The final summation produces the adaptively filtered image. The steerability condition is not restricted to derivative filters and could be expressed for any signal f as:

$$f^{\theta}(x,y) = \sum_{m=1}^{M} k_m(\theta) f^{\theta_m}(x,y) \qquad (3)$$

where $f^{\theta}(x,y)$ is the rotated version of f by an arbitrary angle , $k_m(\ )$ are the interpolation functions, $f^{\theta_m}(x,y)$ are the basis functions and M the number of basis functions required to steer the function $f(x,y)$.

To determine the conditions under which a given function satisfies the steering condition in Eq. (3), let us work in polar coordinates ($r = \sqrt{x^2 + y^2}$ and $\phi = \arg(x, y)$).

The function f could be expressed as Fourier series in polar angle ϕ:

$$f(r,\phi) = \sum_{n=-N}^{N} a_n(r) e^{jn\phi} \qquad (4)$$

where $j=\sqrt{-1}$ and N is the discrete length of coefficients. It has been demonstrated in [6] that the steering condition in

Eq. (3) is satisfied for functions expandable in the form of Eq. (4) if and if only the interpolation function $k_m(\ )$ are solution of:

$$c_n(\theta) = \sum_{m=-1}^{M} k_m(\theta)(c_n(\theta))^m \qquad (5)$$

where $c_{n=} e^{jn\theta}$, and $n=\{0,\ldots, N\}$.

From of Eq.(5), $f^{\theta}(r,\phi)$is expressed as:

$$f^{\theta}(r,\phi) = \sum_{m=1}^{M} k_m(\theta) g_m(r,\phi) \qquad (6)$$

where $g_m(r,\phi)$ can be any set of functions.
It has been also demonstrated that the minimum number M of basis functions required to steer $f(r,\phi)$ is equal to the number of non-zero Fourier coefficients $a_n(r)$.

III. Proposed Corner Detection

We propose new corner detection using the steerable filters[5] and Harris algorithm as follows:
1. Decomposition of an image with different orientations using steerable filters
2. Detect the corners in each direction using Harris algorithm.
3. Combine all detected corners by performing logical or operation.
4. Applying dilation to the combined nearby corners to make them into one.
5. Find the centroid of step 4 and identified as corner.

We propose a corner detection algorithm as shown in Fig 5. that uses the steerable filters. The experiments carried out with matlab make it clear that if the number of orientations is four it gives better localization and minimum number of false corners detection

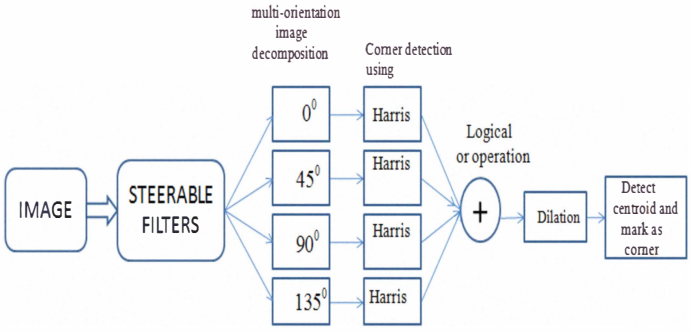

Figure 5 Propose algorithm

IV. Feature Descriptor Extraction

Once the feature points are extracted, each of the feature points is given an "identity". Without the "identity", the feature points are just purely coordinators that indicate where the features are located, and the feature points cannot be matched. Hence, a feature point descriptor is required to generate an "identity" for each of them. A 21x21 feature point descriptor is used in this paper. The "identity" will be usually generated using the information that is obtained from the neighbouring pixels of a feature point.

V. Feature Matching

In this step, the correspondence between feature points, P, in the reference image and feature points, P', in the input image are evaluated. The best candidate match for each feature point is found by identifying its nearest neighbour in the data set of feature vectors from input image. The nearest neighbour is defined as the feature point with minimum Euclidean distance for the invariant descriptor vector.

A. Homography Estimation using RANSAC

Random Sampling Consensus (RANSAC)[7] is an algorithm to fit a model to the data set while classifying the data as inliers and outliers. This algorithm has been applied in estimating the fundamental matrix to match two images with wide or short baseline and estimating a homography. A set of inliers can be determined from an input data set of points. It proceeds as follows:
1. Sample N times from the data set randomly. N is the number of trials required to achieve a confidence level p, which is chosen around 0.9 ~ 0.99
2. Select 4 pairs of sample points and make sure that no three of them are on the same line. Compute $\boldsymbol{H}$ through the sample points.
3. Compute the distance between the matched inliers after the H transformation.
4. Compare the distance with the threshold. If it is less than the threshold, keep the points as inliers. Compute the $\boldsymbol{H}$ from the sub-data-set which contains the most inliers.

B. Image mosaics

After computing the transformation function for each image, we can compose images into one big image. If we stitch the images directly, the blending image will contain obvious boundaries due to the luminance difference. The fade-in and fade-out method can be implemented to reduce the stitched images gap. The value of the pixel in the overlapping image is the weighted average value of the corresponding pixel in the two images.

VI. Experimental Results

In this section we measuring performance in terms of matching score and tested on motion blur images.

A. Blur

Image alignment or registration is a fundamental task for panorama, mosaic and photo stitching applications. However, existing methods are applied only to good images without motion blur[9,10]. During the working process of a camera,

relative motion between the target and the camera will cause motion-blur or camera shake causes blurry photographs. The motion can be controlled by angle or direction and/or by distance in pixels. In this paper, we study the problem of aligning two images; one is blurred and other one non-blurred.

B. Matching score

Performance of mosaic can also be evaluated in terms of the matching accuracy rate and matching score[8]. The matching accuracy per point pair is more important than the quantity of matched pairs. The matching score is computed between the reference image and the sensed image, and computed as follows:

1. Detect number of features in reference and senesced images
2. Find corresponding number of initial matching points using Euclidean distance
3. We finding correct matching points using RANSAC

$$\text{Matching Score} = \frac{\#\text{Correct matching points}}{\#\text{Total matching points}} \quad (7)$$

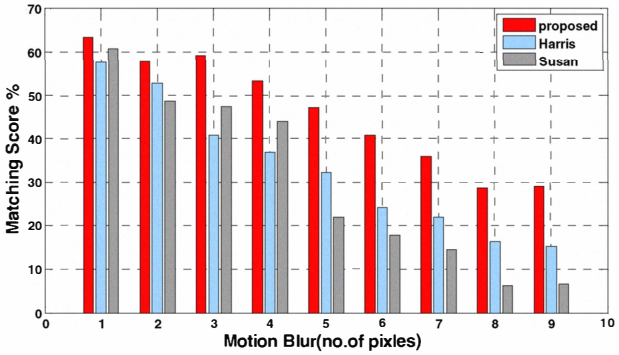

Figure. 6. Matching accuracy rate for motion blur image

First, an image mosaic experiment is conducted with one blurred and one non-blurred images. The blurred image obtained with a pixel distance in steps of 1 pixel variations between 1 and 9 is as shown in Fig 6. It is observed that the performance of proposed method perform better which is indicated with red colour is better between 1 to 9 pixel distances when compared with Harris and Susan methods.

The experiments are carried out and tested on number of building images with different sizes. From the experimental results it can be concluded that the matches obtained are accurate and stable with proposed method. Figs.7 (a), (b) and (c) shows the three input images used for stitching. Fig. 7(d) shows 201 initial matches found. Fig. 7(e) shows 69 correct matches using Harris. Fig. 7(f) shows the mosaic image.

(a) (b) (c)

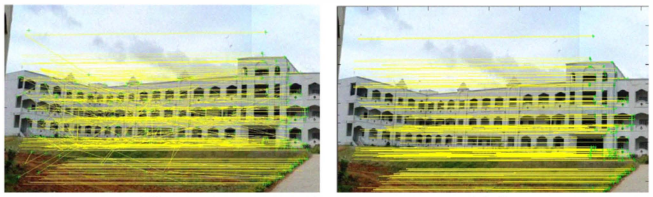

(d) (e)

(f)

Figures. 7(a)-(f). Building image Mosaic Results by using feature points

Fig.8 shows another mosaic process of two Ellora Caves images. Fig.8(a) and Fig.8(b), with sizes of 518 x388, are the images to be stitched. Fig.8(c) and (d), shows 343 initial matches and 249 correct matches respectively using Harris. Fig.8(e) shows the result of image mosaic.

VII. Conclusion

In this paper, the performance of various feature point detectors in extracting feature points is shown. It can be seen that success rate of stitching is strongly related to number of feature points. However, it is not wise to blindly increase the number of feature points that can be extracted by a detector, since it will lead to increase in processing time due to massive amount of matching operation.

In addition, Table I show the numbers of corner points detected, initial match numbers, correct matches and matching score. It is observed that the proposed method performs better matching scores. So it can be concluded that proposed method is effective compared to Harris and Susan corner detection methods.

(a) (b)

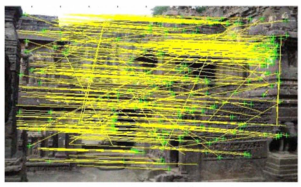

(c)

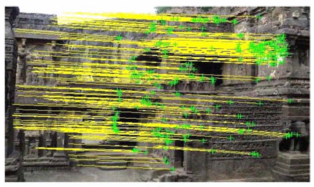

(d)

(e)

Figures. 8(a)-(e). Ellora caves image Mosaic Results by using feature Points

TABLE I
IMAGE MOSAIC RESULTS

Methods	Image size	Number of corners detected	Number of initial matches	Number of correct matches	Matching Score %	Time in sec
Harris	Fig7(a) 512x512	525 437	201	69	34.32	1.567
Susan		1282 831	366	154	42.7	1.589
Proposed	Fig7(b) 512x512	498 408	74	38	51.35	1.790
Harris	Fig8(a) 518x388	908 1066	343	249	72.59	1.771
Susan		4511 5553	730	594	81.369	1.982
Proposed	Fig8(b) 518X388	605 713	58	53	91.37	1.775

REFERENCES

[1] C. Harris, M. Stephens,"A combined corner and edgedetector," in Fourth Alvey Vision Conf., pp. 147-151, 1988

[2] S. Smith, J. Brady,"SUSAN—a new approach to low-level image processing," Int. J.Comput. Vis. 23_1_, pp. 45– 48, 1997.

[3] L. Kitchen, A. Rosenfeld, Gray level corner detection, Pattern Recognit. Lett. 95–102 (1982)

[4] Soo-Hyun CHO , Yun-Koo CHUNG, Jae Yeon LEE "Automatic Image Mosaic System Using Image Feature Detection and Taylor Series" Proc. VIIth Digital Image Computing: Techniques and Applications, 10-12 Dec. 2003

[5] Freeman, W.T., Adelson, E.H.: The design and use of steerable filters. IEEE Trans. Pattern Anal.Mach. Intell. **13**, 891–906 (1991)

[6] Simoncelli, E.P., Freeman,W.T. "The steerable pyramid: a flexible architecture for multi-scalederivative computation"In Second Int'l Conf on Image Proc, vol. 3, pp. 444–447,Washington, DC,October 1995

[7] M. A. Fischler, R. C. Bolles. "Random Sample Consensus: A Paradigm for Model Fitting with Applications to Image Analysis and Automated Cartography", Communications of the ACM, pp. 381- 395,1981.

[8] Qatran, M., Mahar, K. and Ismail, O. "Interest points matching system based On Non-Subsampled Contourlet Transform" 2nd International Conference on Computer Technology and Development (ICCTD), pp: 245 – 249 (Nov 2010)

[9] Alex Rav-Acha , Shmuel Peleg ,"Restoration of Multiple Images with Motion Blur in Different Directions" Proceedings of the Fifth IEEE Workshop on Applications of Computer Vision (WACV'00)

[10] Salem Saleh Al-amri et. al. "A Comparative Study for Deblured Average Blurred Images" (IJCSE) International Journal on Computer Science and Engineering Vol. 02, No. 03, 2010, 731-733